QUASI-FREE SCATTERING[1]

By Tore Berggren
Department of Mathematical Physics, Lund Institute of Technology, Lund, Sweden
and
Helge Tyrén
The Gustaf Werner Institute, University of Uppsala, Uppsala, Sweden

1. Introduction

1.1 *Brief history of quasi-free scattering.*—The first kind of quasi-free scattering reaction to be studied extensively was of the form ${}^{A}Z(p,2p)^{A-1}(Z-1)$, which is then interpreted as a direct knocking out of a proton bound in the ${}^{A}Z$ nucleus by a fast incident proton. That this interpretation of the reaction mechanism is realistic at high energies was first demonstrated by Chamberlain & Segrè (1) and Cladis, Hess & Moyer (2) and later verified by Wilcox & Moyer (3). A more complete utilization of the quasi-free proton-proton scattering reaction was made in 1957 by Tyrén, Maris & Hillman (4). This experiment was designed to make a complete determination of the kinematics of the proton-proton collision which is supposed to take place in the nucleus, and the results not only verified the approximate validity of the direct-interaction interpretation, but also demonstrated that this kind of reaction could be used as a powerful tool for investigating nuclear structure (5), in particular the single-particle aspects of it. Later experiments with incident proton energies above 150 MeV at Chicago (6–10), Harvard (11–13), Harwell (14, 15), Orsay (16–23), and Uppsala (24–29) have confirmed this conclusion. Experiments with other similar reactions such as (p,pd) (30–33), $(p,p\alpha)$ (30, 31, 34–39) and $(\alpha,2\alpha)$ (40) have shown that a similar reaction mechanism is responsible for these reactions at a sufficiently high energy.

With improved experimental technique, increased accuracy, and a large amount of reliable data, it is only natural that the approximate nature of the simple descriptions of nuclear structure and reaction mechanism first proposed should become evident. Various refinements, the first and most important one being that of using distorted waves instead of plane waves for the description of the incident and outgoing fast particles, have been proposed for reconciling theory with experimental fact. Some of these refinements are controversial, and it has not yet been possible to test all of them in a fair and proper fashion since this would involve complicated and extensive computation. Still, the basic picture of the reaction process remains useful as a first approximation and we shall start with an elementary presentation of it and fill in the details in subsequent sections.

1.2 *Elementary treatment of quasi-free scattering.*—Let us consider a system T consisting of two particles B and C with masses M_B and M_C,

[1] The survey of literature for this review was concluded in January 1966.

$M_B + M_C \equiv M_T$. In the case of quasi-free p-p scattering, B represents the nuclear proton and C the residual nucleus (the core). We choose our reference system (the laboratory system) to be at rest relative to the center of mass of T (the target nucleus). If we denote the intrinsic state of motion of the system T by $|j\rangle$, we can write the probability amplitude for the system to be (virtually) dissociated into its constituents B and C with momenta $\hbar\boldsymbol{q}$ and $\hbar\boldsymbol{Q}$, respectively, as

$$\langle \boldsymbol{q}, \boldsymbol{Q} | j \rangle = g_j \left(\frac{M_C}{M_T} \boldsymbol{q} - \frac{M_B}{M_T} \boldsymbol{Q} \right) \delta(\boldsymbol{q} + \boldsymbol{Q}) \qquad 1.$$

The argument of the function $g_j(\boldsymbol{p})$ is the relative momentum, i.e. the momentum canonically conjugate to the separation $\boldsymbol{r}_{BC} = \boldsymbol{r}_B - \boldsymbol{r}_C$ of the particles B and C. The δ function represents the fact that the center of mass of the system is at rest, $\boldsymbol{q} + \boldsymbol{Q}$ being the total momentum of the system. Thus we have

$$\boldsymbol{q} = -\boldsymbol{Q} \qquad 2.$$

The function $g_j(\boldsymbol{p})$ is evidently the momentum representation of the intrinsic or relative motion of the system; because of Equation 2 its argument is simply $\boldsymbol{q}$. The wave function $\psi_j(\boldsymbol{r}_{BC})$ in configuration space is related to $g_j(\boldsymbol{q})$ by a Fourier transformation:

$$g_j(\boldsymbol{q}) = (2\pi)^{-3/2} \int \exp[-i\boldsymbol{q}\cdot\boldsymbol{r}] \psi_j(\boldsymbol{r}) d^3r \qquad 3.$$

We wish to study the reaction $T(A, AB)C$, initiated by a fast particle A with mass M_A (the incident proton in quasi-free p-p scattering). Our aim is to relate this relation to free A-B scattering. To this end we introduce the transition operator T_{AB} from which we can compute the A-B scattering cross section $dQ_{AB}^{\text{free}}/d\Omega$. Let the particles A and B have, initially, momenta $\hbar\boldsymbol{p}$ and $\hbar\boldsymbol{q}$, and assume that because of their mutal interaction they scatter each other, getting final momenta $\hbar\boldsymbol{p}'$ and $\hbar\boldsymbol{q}'$. This is described by the matrix element

$$\langle \boldsymbol{p}, \boldsymbol{q} | T_{AB} | \boldsymbol{p}, \boldsymbol{q} \rangle = \delta(\boldsymbol{p}' + \boldsymbol{q}' - \boldsymbol{p} - \boldsymbol{q}) \langle \boldsymbol{x}' | t_{AB} | \boldsymbol{x} \rangle \qquad 4.$$

where $\boldsymbol{x}$ and $\boldsymbol{x}'$ are the relative momenta of A and B before and after the collision, respectively. We have

$$\boldsymbol{x} = \frac{M_B \boldsymbol{p} - M_A \boldsymbol{q}}{M_A + M_B} \qquad 5.$$

and similarly for $\boldsymbol{x}'$. The δ function in Equation 4 follows from conservation of total momentum in the A-B scattering

$$\boldsymbol{p} + \boldsymbol{q} = \boldsymbol{p}' + \boldsymbol{q}' \qquad 6.$$

The matrix element $\langle \boldsymbol{x}' | t_{AB} | \boldsymbol{x} \rangle$ is proportional to the A-B scattering amplitude in the center-of-mass system of A and B.

If we can neglect, during the short time that A spends near C, the interaction between A and C, and also any momentum transfer from B to C after

B has acquired a large velocity as a result of its interaction with A, then the $T(A,AB)C$ reaction cross section can be calculated in terms of $\langle \boldsymbol{x}' | t_{AB} | \boldsymbol{x} \rangle$ and $g_j(\boldsymbol{q})$ by means of the so-called impulse approximation (41, 42) according to which the transition operator T_{AT} for A-T scattering and reactions is approximated by T_{AB}. Then, if the reaction products A, B, and C have momenta $\hbar\boldsymbol{k}_2$, $\hbar\boldsymbol{k}_1$, and $\hbar\boldsymbol{K}$, and the projectile A has momentum $\hbar\boldsymbol{k}_0$ before the reaction,

$$\langle \boldsymbol{k}_2, \boldsymbol{k}_1, \boldsymbol{K} | T_{AT} | \boldsymbol{k}_0, j \rangle \cong \langle \boldsymbol{k}_2, \boldsymbol{k}_1, \boldsymbol{K} | T_{AB} | \boldsymbol{k}_0, j \rangle = \int \langle \boldsymbol{k}_2, \boldsymbol{k}_1 | T_{AB} | \boldsymbol{k}_0, \boldsymbol{q} \rangle \langle \boldsymbol{q}, \boldsymbol{K} | j \rangle d^3q$$

or, using Equations 1 and 4,

$$\langle \boldsymbol{k}_2, \boldsymbol{k}_1, \boldsymbol{K} | T_{AT} | \boldsymbol{k}_0, j \rangle \cong \delta(\boldsymbol{k}_1 + \boldsymbol{k}_2 + \boldsymbol{K} - \boldsymbol{k}_0) \times \left\langle \frac{M_B\boldsymbol{k}_2 - M_A\boldsymbol{k}_1}{M_A + M_B} \middle| t_{AB} \middle| \frac{M_B\boldsymbol{k}_0 + M_A\boldsymbol{K}}{M_A + M_B} \right\rangle g_j(-\boldsymbol{K}) \qquad 7.$$

Again, the δ function represents conservation of total momentum

$$\boldsymbol{k}_0 = \boldsymbol{k}_1 + \boldsymbol{k}_2 + \boldsymbol{K} \qquad 8.$$

and the reaction cross section is proportional to the square of the remaining factors in the right member of Equation 7. In addition to Equation 8 we have the conservation of energy

$$E_0 = E_1 + E_2 + E_r + E_S \qquad 9.$$

where $E_r = \hbar^2K^2/2M_C$ is the kinetic energy of the recoiling core C, and E_S is the separation energy for B, i.e. the smallest energy necessary to separate B from C. Using Equation 7 one obtains (43) for the cross section $d^3\sigma/dE\, d\Omega_1 d\Omega_2$ for a quasi-free scattering reaction in which B is scattered into a solid angle $d\Omega_1$ around $\boldsymbol{k}_1$ and A into $d\Omega_2$ around $\boldsymbol{k}_2$, with outgoing energies within dE of E_1 and E_2, respectively,

$$\frac{d^3\sigma}{dE d\Omega_1 d\Omega_2} = F_{kin} \frac{d\sigma_{AB}}{d\Omega'} \sum_{av} | g_j(-\boldsymbol{K}) |^2 \qquad 10.$$

Here F_{kin} is a kinematical factor so chosen that the square of the matrix element of t_{AB} can be related to the A-B cross section $d\sigma_{AB}/d\Omega'$ at a suitable energy and angle,[2] and Σ_{av} indicates the usual summation over final states and averaging over initial states. In the simple case of B being bound to C by a spherically symmetric potential V_{BC}, and B as well as C being spinless, the latter operation only yields a factor $(2l+1)^{-1}$, where $\hbar l$ is the angular momentum of B relative to C.

[2] There is an ambiguity in the choice of $d\sigma_{AB}/d\Omega$ because there is in general no real scattering process which corresponds exactly to the matrix element $\langle \boldsymbol{x}' | t_{AB} | \boldsymbol{x} \rangle$, since the relative kinetic energies corresponding to the momenta $\hbar\boldsymbol{x}$ and $\hbar\boldsymbol{x}'$ are in general different in the $T(A, AB)C$ reaction because B is initially bound. At energies which are large compared to the average kinetic energy of B in T, this so-called off-energy-shell effect should be small, however.

Equation 10 is the basis for all quasi-free scattering experiments, since if it holds, it implies that one can study the momentum distribution of the particle B in the target T experimentally by measuring the (recoil) momentum distribution of the residual core C after the reaction.

With a spherically symmetric interaction $V(|\mathbf{r}_{BC}|)$ between B and C, the relative orbital angular momentum $\hbar\mathbf{L}_{BC}=\mathbf{r}_{BC}\times(-i\hbar\nabla_{BC})$ is a constant of motion, just as in the classical case of a central force. If, classically, $\hbar\mathbf{L}\neq 0$, then the classical momentum is nonzero in every point of the classical orbit, and the recoil momentum $\hbar\mathbf{K}$ could never be zero, if B were suddenly knocked out of the system T. This is also true in a quantal treatment, because then the wave function is of the form

$$\psi_{lm}(\mathbf{r}) = R_l(r)Y_{lm}(\theta, \phi)$$

For $q=0$ in Equation 3, the right member would be nonzero only if $l=0$, because otherwise the angular integrations yield zero. Actually, this is true for more general models of the target (44). Thus it is as a rule quite easy to see from the shape of the recoil momentum distribution, whether the particle B is bound in an $l=0$ state to C or not. A more careful analysis actually often yields still more information. Since, classically, in a circular orbit, the product of radius and momentum equals the angular momentum, and the latter is often restricted to a single value in a quantal system, the position of the maximum of the recoil momentum distribution gives a rough idea of the average radius of the wave function for the motion of B relative to C. The recoil momentum distribution is, in fact, quite sensitive to the extension in space of the wave function. This will be discussed in Section 5.1.

The formula 10 with $g(-\mathbf{K})$ defined by Equation 3 is quantitatively a poor approximation because it neglects the fact that the target $B+C$ is, in general, a many-body system so that the incident particle can cause a large number of different reactions. Thus only a fraction of the incident protons give rise to a $(p,2p)$ reaction, and the rest are "lost." We must somehow describe this situation: the optical model (45) provides a useful tool. A complex potential affects a plane wave representing a material particle with definite momentum in the same way that a medium with a complex index of refraction affects a light wave: the wave is refracted and, because of the imaginary part of the potential (or index of refraction), absorbed. With a suitable choice of the optical potential it should therefore be possible to take some average of the incident (or outgoing) particle (or particles) and the core into account. This theory is essentially phenomenological, but the important point is that the parameters to be used (the optical potentials) can, at least in principle, be determined from other experiments.

The influence of the optical potential, which is usually different for the incident and the outgoing particles, is usually taken into account by replacing the plane wave $(2\pi)^{-3/2}\exp(i\mathbf{k}\cdot\mathbf{r})$ by a distorted wave

$$\chi(\mathbf{r}, \mathbf{k}) \equiv (2\pi)^{-3/2}D(\mathbf{r}, \mathbf{k})\exp(i\mathbf{k}\cdot\mathbf{r}) \qquad 11.$$

which is a solution to a Schrödinger equation containing the optical po-

tential; the so-called distortion factors $D(\boldsymbol{r}, \boldsymbol{k})$ defined by Equation 11 approach unity for large values of $|\boldsymbol{r}|$. The factor $\exp(-i\boldsymbol{q}\cdot\boldsymbol{r})$ in Equation 3 can be written, using Equations 2 and 8,

$$\exp[-i\boldsymbol{q}\cdot\boldsymbol{r}] = \exp[-i\boldsymbol{k}_0\cdot\boldsymbol{r}]\exp[-i\boldsymbol{k}_1\cdot\boldsymbol{r}]\exp[-i\boldsymbol{k}_2\cdot\boldsymbol{r}]$$

and then we may assume that in the presence of distorting optical potentials we should replace $g(-\boldsymbol{K})$ in Equation 10 by the so-called distorted momentum distribution (43)

$$g_j'(\boldsymbol{k}_0, \boldsymbol{k}_1, \boldsymbol{k}_2) = (2\pi)^{-3/2}\int \exp[+i\boldsymbol{K}\cdot\boldsymbol{r}]D(r, \boldsymbol{k}_0)D^*(\boldsymbol{r}, \boldsymbol{k}_1)D^*(\boldsymbol{r}, \boldsymbol{k}_2)\psi_j(\boldsymbol{r})d^3r \qquad 12.$$

Experience shows that $|g_j'|^2$ varies with $\boldsymbol{K}$ in almost the same way $|g_j|^2$ does, but the magnitude is different and there may also be a shift in the position of maxima and minima.

It should be possible, then, supposing the validity of the basic assumptions on which the impulse approximation is founded, to extract valuable information on the structure of the target system from quasi-free scattering data, at least if suitable precautions are taken in the planning and performance of the experiment as well as in the theoretical analysis. Since other authors have recently published excellent review articles (29, 46–48) which survey and summarize the results obtained in this field up to 1965, we shall focus our attention on the principles involved in and problems encountered in obtaining, analyzing, and interpreting the data.

2. Problems Involved in Quasi-Free Scattering Experiments

In this section we shall briefly discuss some of the problems involved in quasi-free scattering experiments with emphasis on $(p,2p)$ reactions which have been most extensively studied. Generally such a reaction takes place in a three-dimensional geometry; i.e. the momenta of the incident particle and the scattered particles are not coplanar. In most experiments one detects the scattered particles A and B simultaneously in certain directions relative to the incident beam and at energies E_1 and E_2 which are defined respectively by the acceptance solid angles $d\Omega_1$ and $d\Omega_2$ and the energy channel widths dE_1 and dE_2 of the measuring device. The geometry in which the reaction is observed is thus determined by the experimental setup. Most experiments are performed in a coplanar geometry. A possible additional information which could be obtained from a noncoplanar experiment is discussed in Section 5.2.

The physical nature of the quasi-free scattering reaction imposes certain requirements on the experiment. The energies of the incident particle and the product particles should be sufficiently high so that the range of these particles in nuclear matter is not small compared to the dimensions of the nucleus. The large absorption would otherwise make it difficult to extract useful information from the reaction.

The probability that a fast proton is absorbed should be porportional to the total proton-nucleon cross section. This quantity decreases mono-

tonically with increasing proton energy up to about 200 MeV and then remains roughly constant. In a $(p,2p)$ experiment it should therefore be best to use incident proton energies of 400 MeV or more. At smaller incident proton energies minimum absorption will occur in this reaction if the experiment is performed in a symmetric geometry, i.e. with equal scattering angles and energies. The interpretation of the experimental results and the theoretical treatment is also much simplified in this geometry. If, however, A and B are not identical particles as in reactions of the type (p,pd) and $(p,p\alpha)$ it will be preferable to perform the experiment in a geometry such that the distortions of the scattered particles A and B are not too different. Other kinematical limitations and the role of the absorption are further discussed in Section 5.

The important observables in a quasi-free scattering experiment are the separation energy E_S and the momentum $\hbar\boldsymbol{K}$ of the recoiling core C. They can be determined from measurable quantities by the relations for conservation of energy and total momentum, Equations 9 and 8, respectively, of Section 1. The directions of particles A and B are defined by the positions of the detectors, and the energies E_1 and E_2 are measured in the experiment. The other quantities either are known or can be calculated.

The information which can be extracted from the experiment depends on the accuracy with which the kinematical observables E_S and $\hbar\boldsymbol{K}$ and the cross section $d^3\sigma/(dEd\Omega_1d\Omega_2)$ can be determined. Because the separation energy E_S and the absolute value of the recoil momentum $\hbar\boldsymbol{K}$ are small compared to the energies and momenta of the incident and scattered particles, it is evident from Equations 8 and 9 of Section 1 that the energies and directions of the incident and scattered particles must be accurately measured in the experiment. The solid angles $d\Omega_1$ and $d\Omega_2$ and the channel widths dE_1 and dE_2 within which the energies of particles A and B are measured should therefore be as small as possible. This imposes requirements of a purely technical nature on the quasi-free scattering experiment.

The precision dE_1 and dE_2 is determined by the energy-resolving power of the measuring device. The solid angles $d\Omega_1$ and $d\Omega_2$ may in principle be chosen arbitrarily. However, one must ensure that one measures pairs of particles A and B which are products of the same quasi-free scattering reaction in the target nucleus. With few exceptions this is done by counting the particles in coincidence. In symmetric $(p,2p)$ experiments one counts coincidences at fixed angles for variable equal settings of the energy channels (summed energy spectra), and measures the observed peaks in the summed energy spectra at variable symmetric scattering angles (angular correlation distributions). However, if the energy channel widths dE_1 and dE_2 and the solid angles $d\Omega_1$ and $d\Omega_2$ are small, the probability for accidental coincidences is large. Such coincidences are predominantly due to particles A and B which originate from quasi-free scattering reactions in the target but are not produced in the same nuclear reaction.

For this reason relatively wide energy channels and large solid angles

were used in the original $(p,2p)$ experiments at 185 MeV by Tyrén, Maris & Hillman (4, 24) which were performed with range telescopes in a symmetric coplanar geometry. The number of accidental events was separately measured in these experiments by counting coincidences between pairs of protons produced in adjacent pulses of the beam. In subsequent experiments by Tibell et al. (26–29) the situation was improved by simultaneously counting accidental coincidences and introducing an auxiliary peripheral accelerated electrode in the synchroncyclotron which produces a beam of protons more evenly distributed in time. In the telescope experiment the energy resolution is principally limited by the range straggling of the scattered protons. One will also lose events and measure false events because of inelastic collisions of the protons in the absorbers and the scintillators.

The admixture of accidental events should be less pronounced if the observations are made in a less restricted nonsymmetric geometry. The most complete nonsymmetric $(p,2p)$ experiment was made by Gooding & Pugh (14) at 153 MeV on ^{12}C. They used total energy absorbing plastic scintillators and allowed for all possible combinations of energies and angles. Somewhat similar techniques have been used by Gottschalk & Strauch (11) and by Garron et al. (18). They used total energy absorbing NaI scintillators in a symmetric fixed geometry and observed all possible combinations of protons of energies E_1 and E_2. The results of such nonsymmetric experiments are, however, more difficult to interpret and analyze and the distortion will be large in events where one of the scattered protons has a small energy. In the total absorption scintillators, the energy resolution is defined by the optics and electronics involved in the pulse measurements. Inelastic collisions in the scintillators give rise to numerous false events in these detectors.

A very special technique has been used by Bowden et al. (49) who studied quasi-free scattering reactions in ^{12}C in a bubble chamber. It has the advantage that any three-dimensional event can be observed, but it has limited application.

In more recent $(p,2p)$ experiments by Tyrén et al. at 460 MeV (6–10) and by Ruhla et al. at 155 MeV (20, 21), pairs of magnetic spectrometers have been used to select the momenta of the scattered protons. Particle momenta can be measured with considerable precision in such spectrometers. They do not possess the defects inherent in the range telescopes and the total energy absorbing scintillators, and they discriminate more completely against competing (p,pd) reactions and other reactions. The energy and angular resolution with which the quasi-free scattering experiment can be performed with this kind of instrumentation are mainly limited by the admixture of accidental coincidences. The pair spectrometer set up used at 460 MeV is illustrated in Figure 1. The experiment is performed in a symmetric geometry. The two spectrometers are identical and have four energy channels each. One can make further improvements in the precision of a quasi-free scattering spectrometer experiment by increasing the number of energy channels. This has very recently been done by Arditi et al. (23). They have

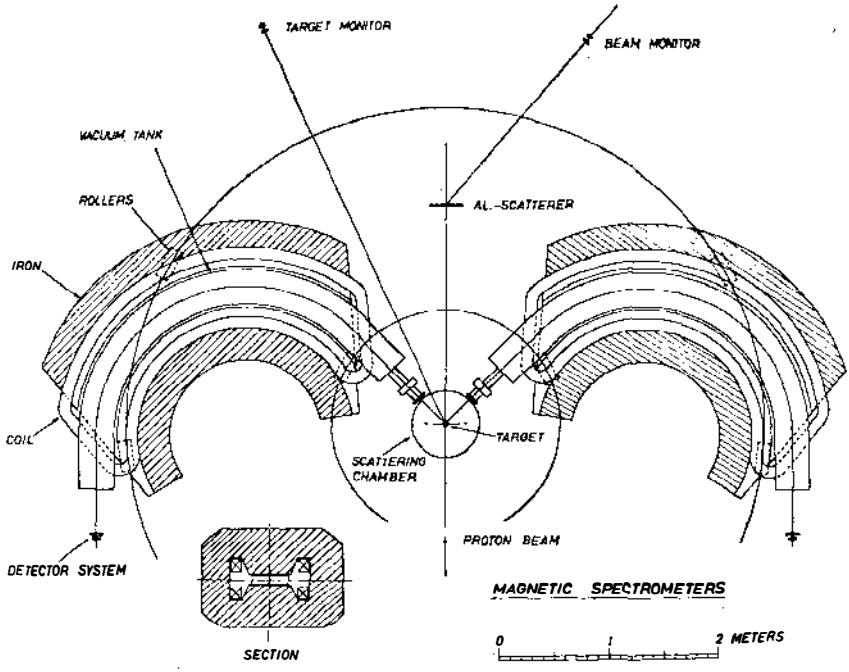

FIG. 1. Magnetic pair spectrometer for momentum analysis used in quasi-free proton-proton scattering experiments at 460 MeV (8–10).

studied $(p,2p)$ reactions at 155 MeV with the previously mentioned spectrometer pair which has been equipped with multichannel spark chamber detectors in the focal region of the spectrometers. A computer on line is used for the data processing. With the 400 MeV proton synchrocyclotron at Liverpool the intent is to study $(p,2p)$ reactions with pair spectrometers and to use spark chambers to define the particle orbits. It will thus be possible to operate with large solid angles because they will have no influence on the definition of the momenta. Accidental coincidences should be negligible in this experiment.

The reliability of the determination of the relative and the absolute cross sections depends on stability conditions and the methods used for monitoring and calibrating the beam. There is some uncertainty as to how accurately the absolute cross sections have been determined in the experiments performed.

Table I, largely taken from (46), shows important experimental parameters in $(p,2p)$ studies. The experiments are listed in chronological order.

A quasi-free scattering reaction of particular interest is the $(e,e'p)$ reaction. The advantage of this reaction compared to the $(p,2p)$ reaction is, as pointed out by Jacob & Maris (50), that the electrons are much less distorted in nuclear matter than the strongly interacting protons. To transfer suffi-

TABLE I

IMPORTANT EXPERIMENTAL PARAMETERS IN $(p,2p)$ STUDIES

Laboratory and references	E_0 (MeV)	Energy detector	Energy resolution (MeV)	Horiz. opening angle	Nuclides studied
Uppsala (4, 6, 24, 25)	185	Range telescopes	4.4	10	^{7}Li, ^{9}Be, ^{11}B, ^{12}C, ^{14}N, ^{16}O
Harwell (14, 15)	150	Total absorption plastic scintillators	6	6.5	^{7}Li, ^{9}Be, ^{12}C, ^{16}O and preliminary results on d-s nuclei
Orsay (16–19)	155	Total absorption NaI scintillators	5	5	^{6}Li, ^{7}Li, ^{9}Be, ^{10}B, ^{11}B, ^{12}C
Harvard (11–13)	160	Total absorption NaI scintillators	7 to 4	3	^{7}Li, ^{9}Be, ^{11}B, ^{12}C, ^{16}O, ^{19}F, ^{45}Sc, ^{51}V, ^{59}Co, ^{58}Ni
Uppsala (26–29)	185	Range telescopes	3	3.3 8.8	^{6}Li, ^{7}Li, ^{9}Be, ^{10}B, ^{11}B, ^{24}Mg, ^{27}Al, ^{28}Si, ^{31}P, ^{40}Ca
Chicago (8–10)	460	Magnetic spectrometers with 4+4 plastic telescopes	3	3.6	^{4}He, ^{6}Li, ^{7}Li, ^{9}Be, ^{10}B, ^{11}B, ^{12}C, ^{14}N, ^{16}O, ^{27}Al, ^{28}Si, ^{31}P, ^{32}S, ^{40}A, ^{40}Ca, ^{51}V, ^{59}Co
Orsay (20–22)	155	Magnetic spectrometers with 30+8 plastic detectors	4 to 2	3.5	^{6}Li, ^{40}Ca, ^{45}Sc, ^{48}Ti, ^{51}V, ^{52}Cr, ^{55}Mn, ^{56}Fe, ^{58}Ni, ^{75}As
Orsay, Oxford (49)	50–130	Bubble chambers			^{12}C
Orsay (23)	155	Magnetic spectrometers with spark chambers	1.6		^{2}H, ^{7}Li, ^{9}Be, ^{22}Na

cient momentum to the bound proton it is necessary to use electrons of relatively high energy. Also, because of the very poor duty factor of existing electron accelerators, one will have considerable admixture of accidental coincidences. To obtain reasonable statistics it will therefore be necessary to use large solid angles and wide energy channels. Johansson (51) studied $(e,e'p)$ reactions in ^{3}H and ^{3}He using 550 MeV incident electrons from the Stanford Mark III linear accelerator. He used two magnetic spectrometers. One of these was used to measure electrons of ~450 MeV in a single energy channel at a fixed angle of ~50° and the other spectrometer measured protons of ~100 MeV in 10 channels at variable angles. Energy spectra and angular correlation distributions were measured in this experiment.

Amaldi et al. (52–55) used 550 MeV electrons from a synchrotron to study $(e,e'p)$ reactions in ^{9}Be, ^{12}C, ^{27}Al, and ^{32}S. The experimental setup is shown in Figure 2. Scattered protons of about 100 MeV are measured in a range telescope at a solid angle of 0.16–1 steradian and the scattered electrons of ~450 MeV are focused by two magnetic quadrupoles, deflected 40° by a magnet, and detected in five energy channels. Spectra are obtained by varying the energy of the incident electrons. The energy resolution is claimed to be 10 MeV, and is thus at present poor in this experiment and the recoil momentum is very badly defined. It seems quite possible, however, that one can improve considerably on this experiment by introducing the techniques recently employed in the $(p,2p)$ experiments discussed above. We shall comment further on some results of this experiment in Section 5.3.

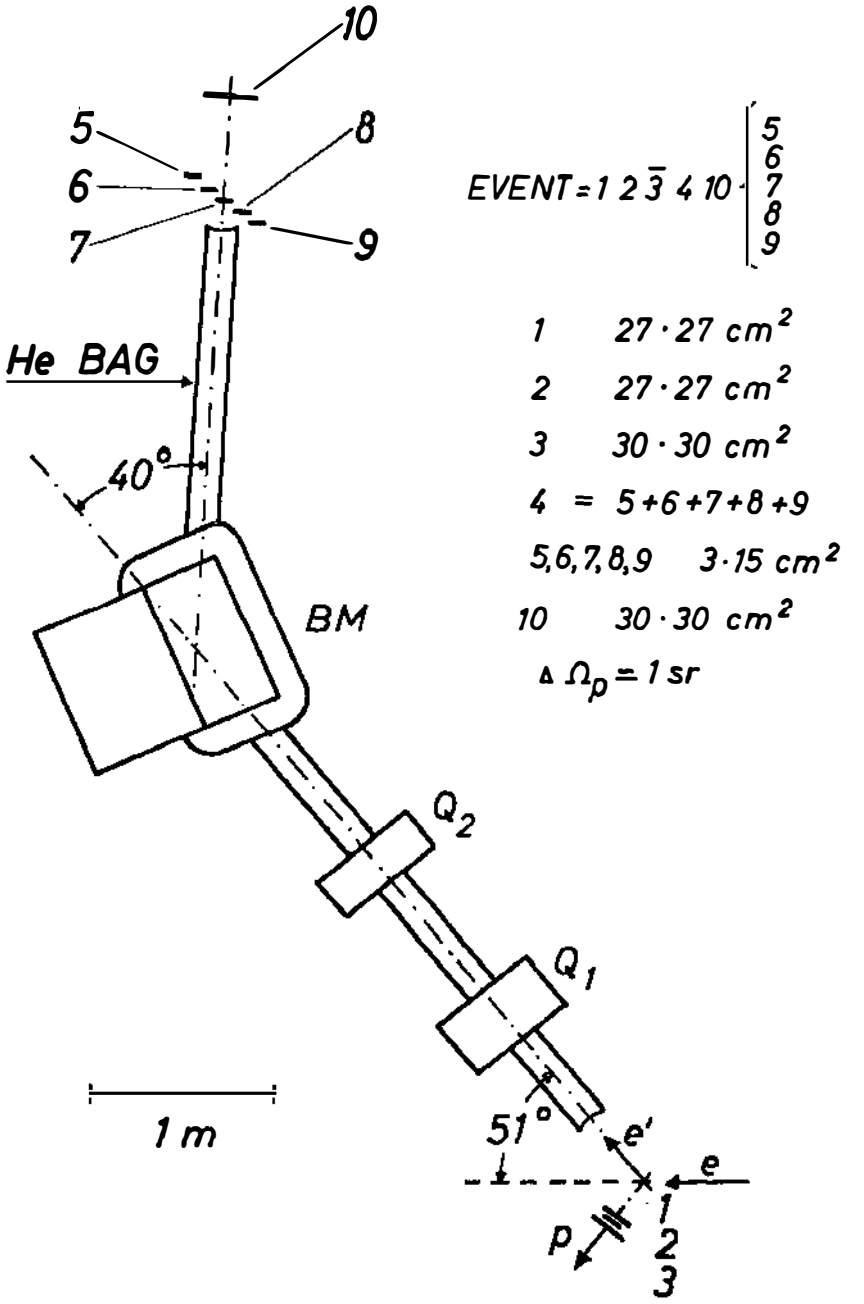

FIG. 2. Experimental setup for quasi-free electron-proton scattering used in experiments at ~550 MeV (52–55).

3. The Dependence on Nuclear Structure

3.1. *The shell-model approach.*—The shell model (56), suggested in the 1930's and improved decisively in 1949 by the introduction of a spin-orbit coupling, was the first really successful description of nuclear structure[3] and in particular of the single-particle properties of nuclei. It is therefore the obvious starting point of any more realistic theory of quasi-free scattering and also of single-particle transfer reactions such as (p,d) and (d,p) reactions. A detailed account of the shell-model formalism is out of the question here; moreover, a comprehensive presentation of the relevant aspects has been given in the *Annual Review of Nuclear Science* by Glendenning (58). It is sufficient to remind the reader that the antisymmetrized wave function for an A-particle state in this model, actually constructed from products of A single-particle wave functions (orbitals), can be formed by a recursive procedure, the so-called fractional parentage expansion (59). Thus if $\Phi_{IM\alpha}{}^{A}(\mathbf{r}_1, \mathbf{r}_2, \cdots, \mathbf{r}_A)$ denotes an A-particle state with prescribed values of the spin I, its projection M and some (set of) additional quantum numbers α, and analogously $\Phi_{JN\beta}{}^{A-1}(\mathbf{r}_2, \cdots, \mathbf{r}_A)$ denotes an $(A-1)$ particle state, and if the single-particle states are denoted $\phi_{nljm}(\mathbf{r})$, where n is the radial quantum number, l the orbital, and j the total angular momentum, and m the projection of j, then the expansion reads

$$\Phi_{IM\alpha}{}^{A}(\mathbf{r}_1, \mathbf{r}_2, \cdots, \mathbf{r}_A) = \sum_{nljJ\beta} F(nljJ\beta; I\alpha) \times \sum_{m} C(jJI; m, M-m)\phi_{nljm}(\mathbf{r}_1)\Phi_{J,M-m\,\beta}{}^{A-1}(\mathbf{r}_2, \cdots, \mathbf{r}_A) \quad 13.$$

Here $F(nljJ\beta; I\alpha)$ is a so-called coefficient of fractional parentage (c.f.p.) and $C(jJI; m, M-m)$ is a Clebsch-Gordan coefficient which effects the coupling of the angular momenta j and J to I. Usually a more special expansion is assumed so that, for instance, all terms have the same n, l, and j (successive filling of the nlj subshell in j-j coupling). In this case one usually employs a notation

$$F(nljJ\beta; I\alpha) \equiv (j^{p-1}jJ\beta \,|\, \}\, jPI\alpha)$$

where p is the number of nucleons in the last unfilled shell of the A-particle nucleus. Such coefficients have been tabulated (60–66) in j-j as well as L-S coupling for several shells.

The implication of this expansion for quasi-free scattering is that the probability amplitude for knocking out a proton at $\mathbf{r}_1$ leaving the residual nucleus in the state $\Phi_{JN\beta}(\mathbf{r}_2, \cdots, \mathbf{r}_A)$ is proportional to the function

$$\psi(\mathbf{r}_1) = \sum_{nlj} F(nljJ\beta; I\alpha)C(jJI; M-N, N) \times \phi_{nlj,M-N}(\mathbf{r}_1) \quad 14.$$

where I, M, α are the quantum numbers of the initial state of the target.

[3] A comprehensive review of current ideas of nuclear structure, especially that of light nuclei, is given by Goldhammer (57).

In a pure j-j or L-S coupling case the sum in Equation 14 reduces to a single term, which is then proportional to a single-particle function $\phi_{nlj,M-N}(r_1)$. But the pure case is seldom a good approximation because it neglects the residual interactions between the nucleons, i.e. that part of the total interaction which is not adequately described by the overall shell-model potential. Instead one should at least use intermediate coupling which implies a diagonalization of the complete Hamiltonian with respect to a suitable set of j-j or L-S coupled shell-model states. The general formula for the quasi-free scattering cross section in this case is given by Dietrich (67) who also indicates how to take the so-called rearrangement effects into account. Those effects, first discussed in this context by Benioff (68), are traceable to the fact that the shell-model potential for the A-particle system is slightly different from that of the $A-1$ particle system because of the self-consistency requirement that is understood to justify the shell model. The single-particle wave functions are therefore not identical in $\Phi_{J_N\beta}{}^{A-1}(r_2, \cdots, r_A)$ and $\Phi_{IM\alpha}{}^{A}(r_1, r_2, \cdots, r_A)$, and this increases, in principle, the number of terms necessary in Equation 14.

The pure shell model predicts qualitatively (5) that the summed-energy spectra in quasi-free scattering should show peaks corresponding to the single-particle states in the shell-model potential with peak areas varying roughly as the occupation numbers of the corresponding shells. The first

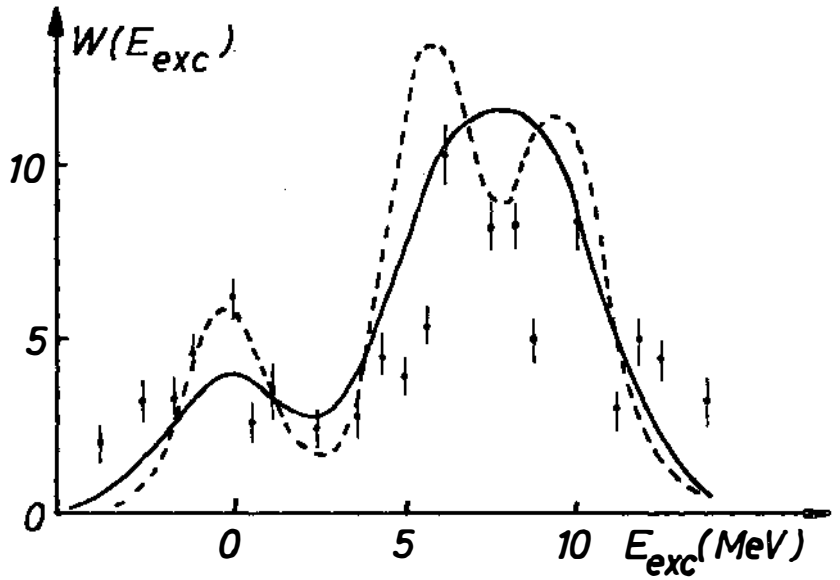

FIG. 3. ^{13}C excitation curves in the reaction $^{14}N(p,2p)^{13}C$ calculated in (69) assuming an experimental resolution of 4.4 MeV (solid curve) or 3.0 MeV (dashed curve). Experimental points from (24).

experiments (4, 24) did in fact agree quite well with these predictions. Intermediate coupling calculations (67, 69, 70) of the spectra are generally in still better agreement with experiment. For technical reasons these early experiments (4, 14, 24) were performed with a rather low angular and energy resolution. The data thus obtained are therefore in fact sums or averages of the reaction cross section over quite large momentum and energy intervals. Hence the detailed structure of the summed-energy spectrum, which sensitively depends on the dynamics of the nucleus, is smeared out as can be seen in Figure 3. Since the shell model mainly aims at deriving the properties of the nuclear states from their symmetry properties under rotation and permutation, avoiding any too special dynamic assumptions, it should be quite adequate for analyzing those data. Accordingly the first predictions of angular correlation distributions of the $^{7}Li(p,2p)^{6}He$ reaction (43, 71) and the $^{12}C(p,2p)^{11}B$ reaction (72, 73) were based on the *j-j* coupling shell model with harmonic oscillator wave functions, and the results obtained were not too seriously in conflict with the experimental data available (4, 14, 24) at the time, considering the uncertainties in the values of the parameters entering the calculation.

When it comes to predicting recoil momentum distributions, however, later experience shows (10, 74–82) that one must abandon the orthodox shell model. The main reason for this is the unrealistic behavior of the shell-model wave functions, especially those of the harmonic oscillator potential, in the outer part of the nuclear surface, and the fact (to be further discussed in Section 5) that most of the quasi-free scattering processes occur in the outer surface region. Another serious drawback of this model is its lack of translational invariance, which leads to spurious states corresponding to excitation of the center-of-mass motion in the fictitious shell-model potential well. Furthermore, the probability amplitude for finding a proton at a certain point in the nucleus obviously cannot depend on the distance of this point from the center of the fictitious well, but must be a function of a relative coordinate, e.g. the position relative to the center of mass of the residual core. Only in the case of harmonic oscillator wave functions can one eliminate the center-of-mass coordinate in a simple way (83): regrettably, these functions are not suitable for quasi-free scattering analysis (75, 76, 81). The single-particle+core model of Section 1, on the other hand, clearly is formulated in a translationally invariant way, and in Section 3.2 we introduce a generalized single-particle wave function.

3.2 *The phenomenological approach.*—The shell-model formalism is highly developed and employs quite powerful tools, mostly of group-theoretical origin, such as the fractional parentage expansion. It fails, however, to yield quantitative agreement in many cases of quasi-free scattering (and other reactions as well), particularly in regard to angular distributions. These often depend sensitively on properties of a more complicated dynamical origin, such as binding energies and radial distributions, and therefore a more phenomenological approach has been suggested (84, 85) and actually practiced in a simplified form in most of the recent calculations.

Since the nuclear quantity of interest in predictions of quasi-free scattering is the probability amplitude of finding a proton with a definite relative momentum or at a definite relative position with respect to the residual nucleus in a particular state (as a rule the final state), one expresses the properties of the nucleus in terms of these amplitudes, which then replace the single-particle wave functions of the shell model. These amplitudes are called invariant wave functions (86), stripping or pickup form factors (85, 87), or overlap integrals (5, 84). A more descriptive term would perhaps be fragmentation amplitude, since it can be defined as the amplitude for a fragmentation of the A-particle nucleus in the state $|\Phi_{IM\alpha}{}^A\rangle$ into a proton with specified relative momentum $\hbar q$ (or relative position r) and spin projection s, and a residual nucleus (or core) in a specified state $|\Phi_{JN\beta}{}^{A-1}\rangle$. We can write these amplitudes as inner products and have the relation (cf. Equation 3)

$$\langle q,\, s,\, \Phi_{JN\beta}{}^{A-1}|\, \Phi_{IM\alpha}{}^A\rangle = (2\pi)^{-3/2}\int \exp\left[-iq\cdot r\right]\langle r,\, s,\, \Phi_{JN\beta}{}^{A-1}|\, \Phi_{IM\alpha}{}^A\rangle d^3r \qquad 15.$$

When possible we shall use abbreviations like $\langle r\beta|\, \alpha\rangle \equiv \langle r,\, s,\, \Phi_{JN\beta}{}^{A-1}|\Phi_{IM\alpha}{}^A\rangle$. Since the kets $|r,\, s,\, \Phi_{JN\beta}{}^{A-1}\rangle$ form a complete set of A-particle states (the center-of-mass coordinate is assumed to be eliminated from the start), we can expand the states $|\Phi_{IM\alpha}{}^A\rangle$ according to

$$\begin{aligned}\langle r_1, r_2, \cdots, r_A|\, \Phi_{IM\alpha}{}^A\rangle &\equiv \langle r_1', r_2', \cdots, r_A'|\, \Phi_{IM\alpha}{}^A\rangle \\ &= \sum_{sJN\beta}\langle r_1', s, \Phi_{JN\beta}{}^{A-1}|\, \Phi_{IM\alpha}{}^A\rangle\chi_s{}^{1/2}(1)\langle r_2', \cdots, r_A'|\, \Phi_{JN\beta}{}^{A-1}\rangle \qquad 16.\end{aligned}$$

where $\chi_s{}^{1/2}(1)$ is a spin eigenfunction for particle 1, and the primes on the coordinate vectors indicate that we have invoked translational invariance to introduce a relative coordinate, e.g. $r_1' = r_1 - \Sigma_{i=1}{}^A r_i/(A-1)$. Equation 16 is a generalization of the fractional parentage expansion (Equation 13), and since it can be shown (10, 84, 85) that

$$\begin{aligned}\langle r_1', s, \Phi_{JN\beta}{}^{A-1}|\, \Phi_{IM\alpha}{}^A\rangle = \sum_{l,j} &C(l\tfrac{1}{2}j;\, M-N-s,\, s)C(jJI;\, M-N,\, N) \\ &\times Y_{l,M-N-s}(\theta\phi)\langle r(l\tfrac{1}{2})jJ:\, I\beta\|I\alpha\rangle \qquad 17.\end{aligned}$$

we see by comparison with Equation 14 that in terms of the fractional parentage coefficient $F(nljJ\beta;\, I\alpha)$ and the shell-model radial wave functions $R_{nlj}(r)$ we can approximately express the radial amplitudes $\langle r(l\tfrac{1}{2})jJ:\, I\beta\|I\alpha\rangle$ as

$$\langle r(l\tfrac{1}{2})jJ:\, I\beta\|I\alpha\rangle = \sum_n F(nljJ\beta;\, I\alpha)R_{nlj}(r) \qquad 18.$$

This expression is approximate because whereas the quantity r here refers to a relative (proton-to-core) distance, it should in an orthodox shell-model expression denote the distance from the proton to the center of the shell-model potential.

A profound difference between the expansions 13 and 16 is that the $A-1$ particle states in Equation 16 are assumed to be exact eigenstates of the $A-1$

particle Hamiltonian H_{A-1}' (the prime again indicates dependence on relative coordinates only). This makes it possible to express the dynamical A-particle problem as a system of equations for the amplitudes $\langle r\beta | \alpha\rangle$, using the relation

$$H_A' = T_1' + H_{A-1}' + \sum_{p=2}^{A} V_{1p}$$

where T_1' is the relative kinetic energy operator for particle 1 and V_{1p} is the interaction between particles 1 and p. One obtains (84, 85), with $E_\alpha{}^A$ and $E_\beta{}^{A-1}$ denoting the energies of the A and the $A-1$ particle states, respectively,

$$(E_\alpha{}^A - E_\beta{}^{A-1})\langle r\beta | \alpha\rangle = -(\hbar^2/2\mu)\nabla_r{}^2\langle r\beta | \alpha\rangle + \sum_\gamma \int \left\langle r\beta \middle| \sum_p V_{1p} \middle| x\gamma \right\rangle \langle x\gamma | \alpha\rangle d^3x \qquad 19.$$

where γ labels the complete set of $A-1$ particle states to which $|\beta\rangle$ belongs. The quantity μ is the reduced mass of the proton-core system. For large values of $r = |r|$ the interaction term in Equation 19 vanishes [as $(Z-1)e^2/r$, $(Z-1)e$ being the charge of the core], hence the asymptotic behavior of $\langle r\beta | \alpha\rangle$ is governed by the separation energy $E_\beta{}^{A-1} - E_\alpha{}^A$. This is generally not true in the shell-model case if the fractional parentage expansion is restricted to include only the lowest possible *nlj* shells. Now the recoil momentum distribution in quasi-free scattering is very sensitive to the behavior of the wave functions in the surface region of the nucleus. This explains why the shell-model wave functions, and in particular the harmonic oscillator ones, have proved inadequate in most cases (8, 75, 76).

As a first step towards an improved wave function one can keep the structure of the shell-model fractional parentage expansion but choose the single-particle wave functions such that their radial behavior at large distances is correctly determined by the separation energy. The expansion coefficients can the be chosen to be, for instance, the c.f.p. of the j-j coupling scheme, or they can be taken as free parameters to be determined in the analysis of the quasi-free scattering experiment. If the number of these coefficients is chosen to be small, the latter procedure should be feasible since the same coefficients also occur in the expressions for other single-particle quantities (10, 84) such as the rms radius; in addition they must satisfy a sum rule because of the normalization requirement. Insofar as the various experimental data are available, one can therefore use the theory sketched in this subsection as a basis for an essentially phenomenological approach. The complexity of the basic system of equations (Eq. 19) for the functions $\langle r\beta | \alpha\rangle$ is forbidding; Pinkston & Satchler have, however, suggested (85) a method of reducing the system to a set of uncoupled equations with state-dependent effective potentials, for which approximate expressions are derived with the shell model as a starting point.

One of the most thoroughly studied quasi-free scattering reactions is $^6\mathrm{Li}(p,2p)^5\mathrm{He}$. The summed-energy spectrum has, as expected in the shell model, two well-separated peaks at separation energies of about 5 and 22

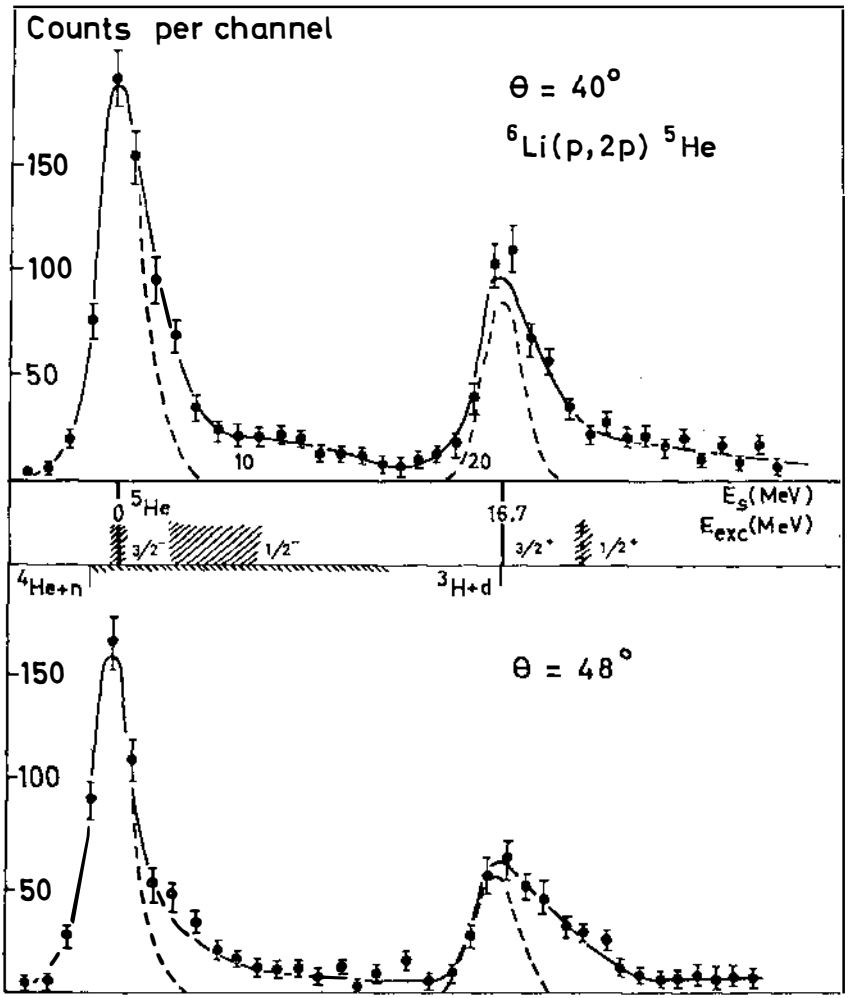

FIG. 4. Summed-energy spectra (from 22) for the ^{6}Li(p,2p)^{5}He reaction. The known ^{5}He spectrum is also drawn. The left-hand peak is interpreted as a 1p and the right-hand peak as a 1s transition.

MeV (see Figure 4) which should be caused by the knocking out of 1p and a 1s proton, respectively. The 22 MeV peak has an angular distribution compatible with this assignment, but the first experiment (16) gave the surprising result that the least-bound protons also appeared to be bound in an $l=0$ orbital. This interpretation was shown to be false on very general grounds (44), even if other nuclear models such as the cluster model (88, 89)

were valid, unless there is a positive parity state close to the $3/2^-$ ground state of ^{5}He. It was also soon found (26) that the angular distribution is so narrow (see Figures. 5 and 6, the experimental points) that a very good angular resolution is necessary to reveal its $l \neq 0$ character. This narrowness indicates a very large radius for the $1p$ orbital in ^{6}Li, but the magnitude of the cross section is almost an order of magnitude smaller than the theoretical cross section (10, 75, 81) for a $1p$ orbital with a radial behavior that yields a reasonable fit to the experimental shape (see Figure 6). This is a striking example of the quantitative breakdown of the shell model. Other, not so flagrant examples are provided by quasi-free scattering in ^{7}Li and ^{9}Be (10, 81).

On the whole, however, one may say that the phenomenologically corrected shell model can explain those features of the recoil momentum distributions obtained in quasi-free scattering which can be attributed to the structure of the target nucleus.

3.3 *Intrinsic widths of the parent states and the problem of continuum states.*—The peaks in the summed-energy spectrum obtained in a quasi-free scattering experiment have, as a rule, a finite width which is partly a consequence of the finite energy resolution ΔE of the experimental equipment but is also, in many cases, a consequence of other circumstances. The experimental resolution can be separately determined by measurement, or calculation, or both, and then taken into account when analyzing the data.

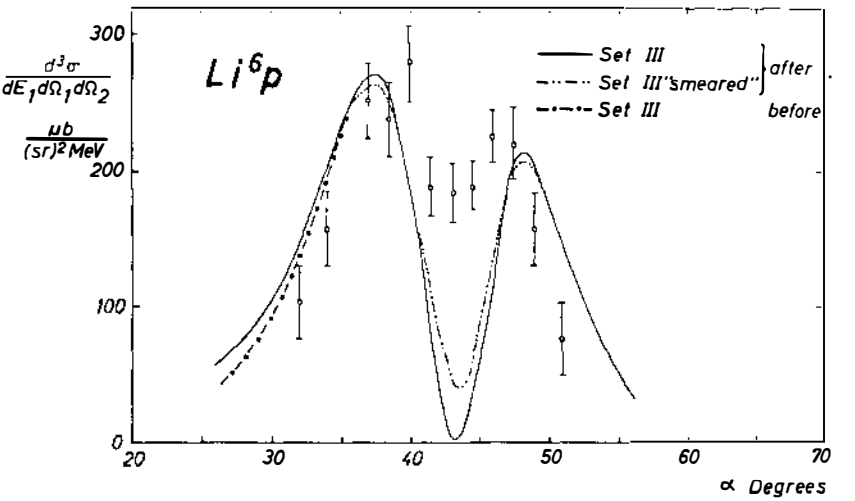

FIG. 5. Angular correlation distribution for the ^{6}Li$(p,2p)^5$He ground state to ground state transition. The experimental results are those of (26, 29). The curves are calculated in (79); the solid and dash-dotted ones are calculated with slightly different treatment of the off-energy-shell effects; the third one shows the effect of finite angular resolution.

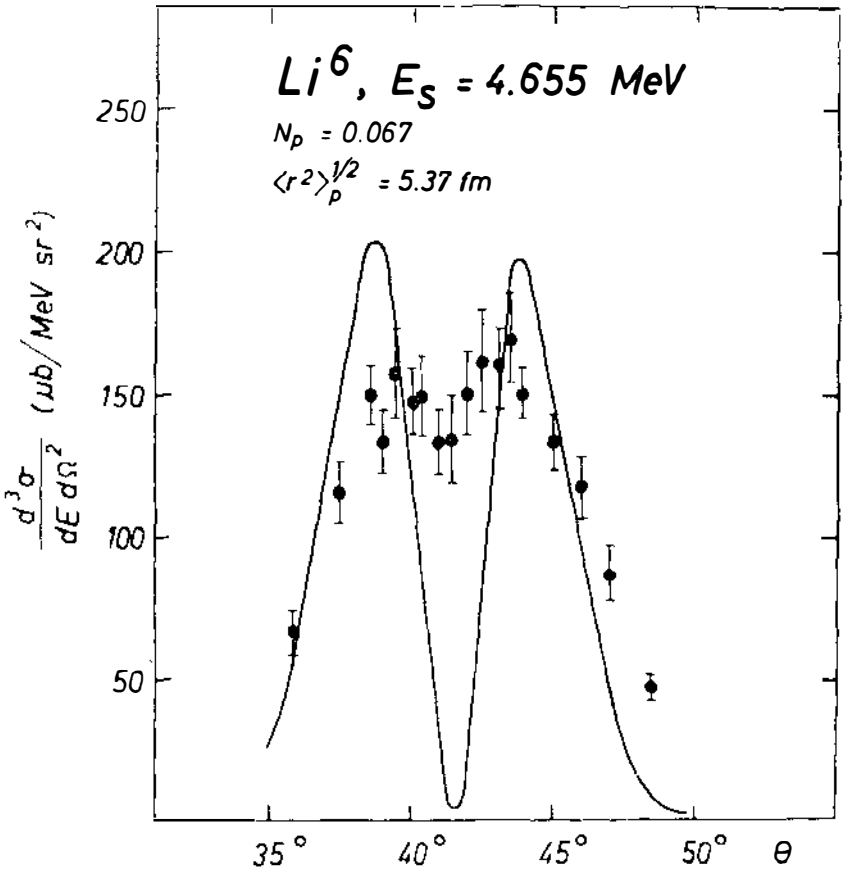

FIG. 6. Angular correlation distribution for the ^{6}Li(p,2p)^{5}He ground state to ground state transition according to (10). The 1p shell radius assumed in calculating the solid curve is larger than that used for the curves in Figure 5, resulting in a better fit to the shape, but it yields a value of the absolute cross section about 15 times the experimental one.

The observed width Γ_{obs}, not due to finite energy resolution, can then be explained either by the fact that two or more final states are so close together in energy that they are not resolved or by the fact that the final state $|\Phi_{JN\beta}{}^{A-1}\rangle$ is isolated but has an intrinsic width $\Gamma_{J\beta}$ because it is a decaying state with a fairly short lifetime $\hbar/\Gamma_{J\beta}$. (If the width is nonzero but $\ll\Delta E$, in this context we consider the state to be sharp.) If the separation energy of the state is not too much larger than that of the ground state of the residual nucleus, one can often identify the final states attained in the reaction and explain the observed widths as being due to unresolved contributions from several states. It is likely that a similar explanation can be found

for many of the widths observed in transitions to highly excited states which, in shell-model terms, are due to the knocking out of a proton from an inner shell, e.g. the $1s$ shell in $1p$ shell nuclei and the $1s$ and $1p$ shells in $2s$-$1d$ shell nuclei. Thus in $^{9}Be(p,2p)^{8}Li$ two final states reached by $1s$ transitions have actually been resolved (10) and probably also in $^{6}Li(p,2p)^{5}He$ (22) (see Figure 4). However, as emphasized by Maris (90), in the case of the inner shells one may also expect a considerable intrinsic width, and Jacob & Maris (47) have estimated this width to be roughly proportional to the number of proton-nucleon pairs in the shell or shells above the shell in question, and inversely proportional to the nuclear volume.

A theoretical determination of the width of an unstable state, or equivalently the imaginary part of the energy of that state, is in principle analogous to a calculation (by perturbation theory or otherwise) of a real energy eigenvalue but may be conceptually and mathematically more intricate because the wave function for such a state increases with distance (91). This circumstance is probably also of importance for the calculation (92) of the real part of the energy eigenvalue corresponding to these excited states. In $^{27}Al(e,e'p)^{26}Mg$ a separation energy of about 60 MeV has been measured (53, 54), and this value is considerably greater than the probable depth (40 or 50 MeV) of the shell-model potential for this nucleus.

Another, somewhat related, problem is the possibility of a transition to the continuum states of the residual nucleus. Since it would seem unphysical to assume that the final state of the residual nucleus could contain any incoming waves, the theory of Humblet & Rosenfeld (91) would imply that only a discrete set of final states, namely, the resonant (or radioactive) states as well as the bound states, would be possible below the threshold for breakup of the residual nucleus into three or more fragments. A true continuum would then be possible only above this threshold, regardless of the reaction mechanism. An apparently continous background due to nondirect (multiple scattering) processes could, however, be superimposed on the quasi-free scattering spectrum since one may expect such processes to excite states of the residual nucleus more complicated than those which occur with large weight in the generalized fractional parentage expansion of the target nucleus (4, 5).

4. The Dependence on the Reaction Mechanism

4.1. *Formal separation of direct and nondirect contributions to the reaction amplitude.*—In this subsection we shall sketch how to use formal scattering theory (93–96) to separate the reaction amplitude into two parts, one of which depends strongly on the interaction between the projectile and the bound particle which is knocked out, whereas the other part proves to be independent of this interaction.

We start from the well-known expression for the transition amplitude M_{ba} for a reaction leading from an eigenstate $|a\rangle$ of an initial interaction-free Hamiltonian H_i, to an eigenstate $|b\rangle$ of a final interaction-free Hamiltonian H_f:

$$M_{ba} = \langle b | V_f | \psi_a^{(+)} \rangle = \langle \psi_b^{(-)} | V_i | a \rangle \qquad 20.$$

In this expression which is valid if the states $|b\rangle$ and $|a\rangle$ have the same energy E, say, the operators V_i and V_f are the sums of all interactions between the particles, elementary or composite, which are considered as free in the initial and in the final state, respectively. The state $|\psi_a^{(+)}\rangle$ and $|\psi_b^{(-)}\rangle$ are scattering eigenstates of the total Hamiltonian $H = H_i + V_i = H_f + V_f$, which satisfy the Lippmann-Schwinger equations (93, 94)

$$\begin{aligned} |\psi_a^{(+)}\rangle &= |a\rangle + (E + i\epsilon - H_i)^{-1} V_i |\psi_a^{(+)}\rangle \\ \langle\psi_b^{(-)}| &= \langle b| + \langle\psi_b^{(-)}| V_f (E + i\epsilon - H_f)^{-1} \end{aligned} \qquad 21.$$

where the infinitesimal quantity ϵ serves to determine the proper asymptotic behavior of $|\psi_a^{(+)}\rangle$ and $\psi_b^{(-)}\rangle$ at infinity (outgoing and incoming waves, respectively).

In quasi-free scattering we have $V_i = V_0 + V_{01}$ with V_0 denoting the interaction between the projectile 0 and the core, and V_{01} the interaction between the projectile and the bound particle 1. With V_1 denoting the interaction between the bound particle and the core and T_0, T_1, and T_C the kinetic energy operators of the projectile, the bound particle, and the center of mass of the core, respectively, and with $H_C \equiv H_{A-1}'$ (cf. Section 3.2), the intrinsic Hamiltonian of the core, we have

$$\begin{aligned} H_f &= T_0 + T_1 + T_C + H_C = H_i - V_1 \\ V_f &= V_0 + V_1 + V_{01} \end{aligned}$$

If we introduce the state $|\chi_a^{(+)}\rangle$ which satisfies

$$|\chi_a^{(+)}\rangle = |a\rangle + (E + i\epsilon - H_i)^{-1} V_0 |\chi_a^{(+)}\rangle \qquad 22.$$

it is easy to apply the formalism of Gell-Mann & Goldberger (94) to rewrite the transition amplitude, Equation 20, in the form

$$\begin{aligned} M_{ba} &= \langle\psi_b^{(-)}| V_0 + V_{01} |a\rangle \\ &= \langle\psi_b^{(-)}| V_{01} |\chi_a^{(+)}\rangle + \langle\lambda_\beta^{(-)}| V_0 |\chi_a^{(+)}\rangle \end{aligned} \qquad 23.$$

where the state $|\lambda_b^{(-)}\rangle$ which is defined as

$$\langle\lambda_b^{(-)}| = \langle\psi_b^{(-)}| - \langle\psi_b^{(-)}| (V_0 + V_{01})(E + i\epsilon - H_i)^{-1}$$

can be shown to satisfy

$$\langle\lambda_b^{(-)}| = \langle b| + \langle\lambda_b^{(-)}| V_1 (E + i\epsilon - H_f)^{-1}$$

Evidently this state is independent of V_{01}. Thus in Equation 23 we have accomplished a separation of the reaction amplitude into one term which depends strongly on the direction interaction V_{01}, namely

$$M_{ba}^{\text{dir}} = \langle\psi_b^{(-)}| V_{01} |\chi_a^{(+)}\rangle \qquad 24.$$

and a nondirect term which is independent of V_{01}. The processes described by the nondirect term must be pictured as multiple collisions in which the projectile 0 first collides with one of the core nucleons which then interacts more or less directly with the extra-core particle 1. To interfere strongly with the quasi-free scattering processes, the momentum transferred in this sequence of collisions must be large, and obviously the amplitude for this kind of process is very small at the energies used in such experiments.

Now let us introduce, in analogy to Equation 22, the state $\langle\chi_b^{(-)}|$ which satisfies

$$\langle\chi_b^{(-)}| = \langle b| + \langle\chi_b^{(-)}| (V_0 + V_1)(E + i\epsilon - H_f)^{-1} \quad 25.$$

Then one can show that

$$\langle\psi_b^{(-)}| = \langle\chi_b^{(-)}| [1 + V_{01}(E + i\epsilon - H)^{-1}]$$

and hence, from Equation 24,

$$M_{ba}^{\text{dir}} = \langle\chi_b^{(-)}| \tau_{01} |\chi_a^{(+)}\rangle \quad 26.$$

with the operator τ_{01} defined by

$$\tau_{01} \equiv V_{01} + V_{01}(E + i\epsilon - H)^{-1}V_{01} \quad 27.$$

In Equation 26, the states $|\chi_a^{(+)}\rangle$ and $\langle\chi_b^{(-)}|$ are the true distorted incoming and outgoing states, respectively, and τ_{01} is the true transition operator describing how the projectile is scattered by the bound particle while both particles interact with the core through the potentials V_0 and V_1 in the Hamiltonian H in the energy denominator of Equation 27.

Even if we could treat the core as an elementary particle, the calculation of the matrix element M_{ba}^{dir}, Equation 27, involves at least one three-body problem, viz. Equation 25, which describes how the motion of the two fast outgoing particles is affected by their interactions V_0 and V_1 with the core. Thus the motions of the free particles in the final states are coupled (80, 82, 97, 98) and the customary factorization of the final distorted wave is not strictly correct, the error being of the order $1/A$. The diproton model proposed by Jackson (98) has an advantage in this respect since it fully utilizes the analogy between (p,d) and $(p,2p)$ reactions and the symmetry of the final state in the latter case. Thus this model allows a more efficient approximate reduction of the three-body problem to two (coupled) two-body problems (the intrinsic motion of the diproton and the distortion of its center-of-mass motion).

The transition operator τ_{01} is also a difficult object, largely because of its dependence on the particle-core interactions V_0 and V_1. At high energies E, however, theory (41, 42, 95) and experience have shown that a fairly good result is obtained by neglecting these interactions, a procedure known as the impulse approximation (41, 42). The operator t_{01} thus obtained

$$t_{01} = V_{01} + V_{01}(E + i\epsilon - H_f - V_C)^{-1}V_{01} \quad 28.$$

differs only kinematically (the presence in H_f of the term H_c which commutes with T_0, T_1, T_C, and V_{01}) from the operator which describes the scattering of the projectile 0 by the free particle 1. The plane-wave matrix elements of t_{01} are therefore diagonal in the core states and proportional to the free scattering amplitudes. Since these matrix elements are functions of the momenta whose variation is relatively slow as compared to the momentum dependence of the distorted waves $|\chi_a^{(+)}\rangle$ and $\langle\chi_b^{(-)}|$, it is usually reasonable to factorize matrix element M_{ba}^{dir}, Equation 26, by extracting the plane-wave matrix element of $t_{01} \simeq \tau_{01}$ that we obtained in Section 1.2, Equation 7, so that

$$M_{ba}^{\text{dir}} \cong \left\langle \frac{M_1 k_2 - M_0 k_1}{M_0 + M_1} \right| t_{01} \left| \frac{M_1 k_0 + M_0 K}{M_0 + M_1} \right\rangle \langle \chi_b^{(-)} \mid \delta(r_0 - r_1) \mid \chi_a^{(+)} \rangle \qquad 29.$$

Although this looks like a zero-range approximation because of the δ function in the second factor, the circumstances that the first factor depends on the initial and final momenta $\hbar k_0$, $\hbar k_1$, and $\hbar k_2$ in the same way as in the case without distortion but with a realistic finite-range transition operator t_{0p}, are arguments indicating that Equation 29, as emphasized by Maris (99), is much better than a zero-range approximation. Calculations by Lim & McCarthy (100–102) have given additional support to the validity of this approximation, at least for incident proton energies larger than 150 MeV.

4.2 *The influence of the distortion on the cross section.*—The interactions V_0 and V_1 between the core and the projectile and the bound proton, respectively, are in principle, assuming for simplicity only two-body forces, sums of projectile-nucleon (V_{0j}) or proton-nucleon (V_{1j}) potentials,

$$V_0 = \sum_{j=2}^{A} V_{0j}, \qquad V_1 = \sum_{j=2}^{A} V_{1j}$$

However, even if the nucleon-nucleon force were known in detail, it could not be used in practice to compute the distorted incoming and outgoing waves $|\chi_a^{(+)}\rangle$ and $\langle \chi_b^{(-)}|$, Equations 22 and 25, because of the many-body problems involved. Therefore the practical procedure is to employ an approximate average interaction, the optical potential, which is complex in order to describe "absorption" (cf. Section 1.2) and, as a rule, energy dependent.

The mathematical form of the optical potential is usually chosen as a compromise between what is physically plausible and what is mathematically convenient. According to the lowest-order approximations obtained by means of multiple scattering theory (95, 103), the shape should be similar to that of the nucleon density in the nucleus. The strength can be determined phenomenologically by analysis of elastic or inelastic scattering experiments, or can be calculated approximately from the projectile-nucleon or proton-nucleon interactions using the methods of Kerman, McManus & Thaler (95).

Having determined the optical potentials $\overline{V}_0^i$ and $\overline{V}_0^f$, $\overline{V}_1^f$ to be used for the computation of the initial (i) and final (f) distorted waves, we can use standard methods to perform these calculations (at least if the three-body character of the final state can be neglected; cf. Section 4.1). The most general one of these methods is the partial-wave method, which has been used by Lim & McCarthy (80, 82) and Jackson & Berggren (97); the latter reference gives a detailed derivation of the formulae involved. Although in principle exact, apart from the physical approximation involved in using the optical model, this method may in practice suffer from a considerable truncation error, especially at high energies, as a result of the necessity of using only a finite number of terms in the partial-wave expansions. Therefore this method may be very expensive in terms of computing time in the analysis of quasi-free scattering at high incident energies, for which the physical errors in the distorted-wave impulse approximation (Equation 29) are expected to be small.

On the other hand, the semiclassical high energy approximation (104), also known as the WKB or eikonal approximation, improves with increasing incident and outgoing energy. In this approximation, the distortion factor $D_{k_0}(\mathbf{r})$ of Equation 11, for the incident particle is given by

$$D_{k_0}(\mathbf{r}) \cong \exp\left\{-i\frac{M_0}{\hbar v_0}\int_{-\infty}^{0}\overline{V}_0{}^i(\mathbf{r}+s\mathbf{k}_0/|\mathbf{k}_0|)ds\right\}$$

where M_0 is the mass and v_0 the velocity of the incident particle. Similar expressions are used for the other distortion factors. For simple shapes of the optical potentials $\overline{V}(r)$ such as square-well Gaussian potentials, the calculation of the distortion factors is quite a simple matter. A comparison between partial-wave and semiclassical treatment (97) has shown that for an incident energy of 185 MeV and Gaussian potentials with a central depth of 30 or 40 MeV, the discrepancy in the predicted quasi-free scattering cross section is at most of the order of 20 per cent.

4.3 *Other possible effects.*—As already mentioned, the optical model takes only the average interaction between the core and the incident or outgoing fast particles into account. In particular it neglects the possibility that the projectile, in addition to knocking out a bound particle, excites the residual core or, similarly, that one of the fast final particles excites or de-excites the core through the particle-core interaction. Since it is impossible to distinguish such a process experimentally from a simpler direct process with the same initial and final states, there will be some interference between them, resulting in a distortion of the observable recoil momentum distribution. The magnitude of the amplitude of such a process can be estimated in the semiclassical approximation insofar as it is due to the distortion, but unless that part of the effective particle-core interaction which can lead to excitation of the core is very strong compared to the optical potential, this effect is found to be small.

However, as we saw in Section 4.1, the true transition operator τ_{01} is also dependent on V_0 and V_1 and so this operator is not diagonal with respect to the eigenstates of the residual core, in contrast to the operator t_{01}, used in practice. Therefore some of the processes just described are due to this nondiagonality. As shown in reference (95) the magnitude of the terms with excited intermediate states, whether due to deviations from the optical potential or to the impulse approximation, depends on the relative importance of two-particle correlations in the target.

A third respect in which the distorted-wave impulse approximation may deviate from reality is the possibility that the interaction between two nucleons is strongly affected by the presence of other nucleons, i.e. the meson exchange between the nucleons is disturbed. This is clearly related to the problem of the existence and magnitude of many-body forces in nuclei. Lim & McCarthy (100, 102) have made calculations which may indicate that the one-pion exchange term is significantly different in the effective interaction to be used in quasi-free $p-p$ scattering from that used in ordinary $p-p$ scattering, at least for low incident energies. However, in view of the long chain

of approximations that led us to the current form (Equation 29) of the distorted-wave impulse approximation there may, of course, be other explanations of the observed deviations which are more serious for low energies where the pure quasi-free scattering interpretation of the reaction is rather doubtful.

The experience gained in the analyses (10, 74–82) of high energy (p, $2p$) reactions with the aid of the distorted-wave impulse approximation as given by Equation 29 shows that one can indeed use this approximation to extract quantitative information (dominant angular momentum, root mean square radius, and effective occupation number [or spectroscopic factor] of the corresponding orbital) concerning the single-proton wave functions of the target nucleus studied. This is true because the approximation reproduces the main features of the angular correlation distributions (position of the maxima and the minima and the overall magnitude) sufficiently well so that effects which are probably due to more complicated distortion processes or to finite experimental resolution can be recognized and taken into account. Alternatively, if the relevant aspects of nuclear structure were known, the effects of the reaction mechanism could be studied in more detail (80, 82, 100, 101).

5. The Problem of Observation of Inner Shells

5.1 *Kinematical limitations on the observability of inner shells.*—Whether we use light or particles as "illumination" for observing a small object, we cannot see details smaller in linear extension than the wavelength used. In quasi-free scattering one has to apply this principle twice. First, in order to distinguish a single nucleon in the target, the reduced de Broglie wavelength of the projectile must be small compared to the average nucleon-nucleon distance in the target. This puts an approximate lower limit on the incident energy (~100 MeV for protons, ~300 MeV for electrons). Secondly, on the assumption that the plane-wave impulse approximation Equation 10 is reasonably true, the momentum $\hbar|\boldsymbol{K}|$ transferred to the residual nucleus is obviously the probe used to observe the single-particle wave function, and hence for a given largest value $K_{\max}$ of $|\boldsymbol{K}|$ we can study in detail only features of this wave function having a linear extent $>(K_{\max})^{-1}$. Since the quasi-free scattering cross section is large only for $|\boldsymbol{K}| \lesssim 1\ F^{-1}$, it is clear that the shape and magnitude of the cross section are mainly sensitive to the large-scale behavior of the wave function. Thus, even if nothing prevented the incident particle from penetrating into the target nucleus or the outgoing particles from escaping, the wave properties of matter would make it necessary to perform very careful analyses of very accurate experiments in order to extract any detailed information on the behavior of the wave functions inside the nuclear surface.

A more formal and quantitative way of describing how the interior of the nucleus is kinematically screened even in the absence of any absorption is the following. Assume for simplicity a wave function for the bound particle of the form $\psi(r) = R_l(r)\, Y_{lm}(\theta, \phi)$, and use the well-known partial-wave expansion of the plane-wave factor in Equation 3, namely

$$\exp\,[i\boldsymbol{q}\cdot\boldsymbol{r}] = (4\pi)^{1/2}\sum_{l'=0}^{\infty} i^{l'}(2l+1)^{1/2} j_{l'}(qr)\,Y_{l'0}\,(\theta,\phi)$$

which, owing to the orthonormality of the spherical harmonics, yields

$$g_l(q) = (\pi\sqrt{2})^{-1}(2l+1)^{1/2}\int_0^{\infty} j_l(qr)R_l(r)r^2dr \qquad 30.$$

The sensitivity of $g_l(q)$ to a change $\delta R_l(r)$ at radius r of the radial wave function is best characterized by the functional derivative $\delta g_l(q)/\delta R_l(r)$ which is defined by the equality

$$\delta g_l(q) \equiv \int_0^{\infty} [\delta g_l(q)/\delta R_l(r)]\delta R_l(r)dr$$

and therefore, by variation of $R_l(r)$ in Equation 30,

$$\delta g_l(q)/\delta R_l(r) = (\pi\sqrt{2})^{-1}(2l+1)^{1/2} j_l(qr)r^2$$

For small values of $q = |\boldsymbol{K}|$ this function behaves near $r=0$ as r^{l+2} and has a first broad maximum at a distance from $r=0$ which increases with decreasing values of q. (For large values of q the oscillatory behavior of $j_l(qr)$ is more important.) Thus for small and moderate values of the recoil momentum $\hbar|\boldsymbol{K}|$ there is a radial localization of the quasi-free scattering reaction to the surface region of the target nucleus for purely kinematical reasons.

5.2 *The role of the absorption.*—It was realized from the beginning of the quasi-free scattering experiments (4, 5) that the absorption in the nucleus reduces the cross section considerably. Semiclassical arguments show (105–111) that this reduction for an individual process is strongly dependent on where in the nucleus the collision between the incoming and the bound particle takes place, and so the absorption leads to a more or less pronounced spatial localization of the reaction. The radial localization of the quasi-free scattering reaction to the surface region of the nucleus is thus enhanced by the absorption, and in addition the bulk of the nucleus will screen parts of its surface from contributing to the process, i.e. there must be a considerable amount of angular localization due to absorption. Some effects of such a localization have been discussed by McCarthy et al (105, 106, 109) and Benioff (110, 111), and more recently Jackson (98) has re-examined this problem in the diproton model. One should keep in mind that in order to be noticeable in the recoil momentum distribution, the localization must have a fairly large extension in space, for the reasons discussed in Section 5.1.

As noted by Jacob & Maris (107, 108) there are, in a coplanar quasi-free scattering experiment, two regions of the nucleus that are not appreciably affected by the absorption of either the incoming or the outgoing particles, namely the polar caps of the nucleus, defined with respect to an equatorial plane parallel to the scattering plane. These polar caps should therefore be the main sources of the outgoing waves, and since they are evidently coherent with a phase difference determined by the symmetry properties of the wave function of the bound particle, one may in favorable cases expect to find a diffraction pattern in the cross section of the scattering geometry is

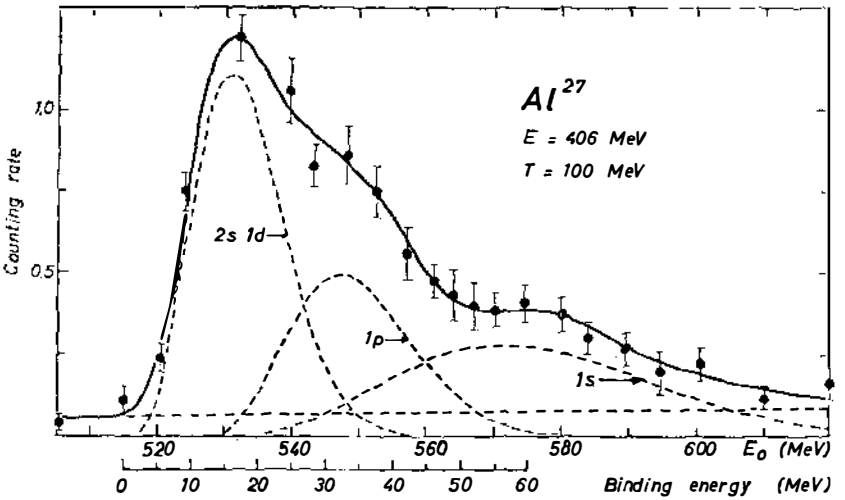

FIG. 7. Summed-energy spectrum of the $^{27}Al(e,e'p)^{26}Mg$ reaction (53, 54).

varied from a coplanar to a noncoplanar situation. From this diffraction pattern, information about the extent of the polar caps and their mutual distance may be obtained. So far only one attempt (27) has been made to verify these predictions. The negative outcome of the experiment should be taken as only an indication that the target nucleus in question (^{40}Ca) is not suited for the experiment which was actually proposed for medium and heavy nuclei, where the polar caps should be better defined and further separated from each other. For the light nuclei, ordinary distorted-wave theories should be applied (72, 73, 98, 112), and there one may not expect any spectacular new phenomenon to occur when going from a coplanar to a noncoplanar situation, since the recoil momentum is the quantity that dominates the shape of the cross section.

5.3 *The relative merits of protons and electrons as projectiles in quasi-free scattering.*—As first suggested by Jacob & Maris (50), the use of electrons as projectiles in quasi-free scattering should offer a clear advantage over the use of protons because the electron is not absorbed by the nucleus. The effect of absorption on a proton is quite serious even at high energy; a theoretically expected reduction of the cross section by an order of magnitude is not uncommon, in particular for inner shells in all nuclei except the lightest ones.

The main drawbacks with the electron are the smallness of the electron-proton cross section and the fact that this cross section varies strongly with the momentum transfer. In addition, at the energies necessary (200–1000 MeV) it is difficult, at least with the techniques used to date, to obtain a good energy resolution. Still, experiments have been initiated at several laboratories (51–55) and promising results have been obtained. Thus, for

example, it has been possible to observe the $1p$ and $1s$ shells in ^{27}Al, in addition to the $2s$-$1d$ shell (Figure 7). It is hoped that these experiments can be developed so as to obtain a good angular and energy resolution.

6. Concluding Remarks

In this article we have tried to describe the present situation and indicate some current trends in the field of quasi-free scattering on single protons in nuclei. Our selection of topics and the emphasis on the various problems that have been discussed are to a large extent determined by the facts that most of the experimental and theoretical results are concerned with incident protons having a kinetic energy above 150 MeV and that this is the energy region in which the interpretation and analysis of the phenomena observed is relatively simple and unambiguous. Thus the $(p,2p)$ work performed and in progress (113–116) at relatively low incident energies ($\sim$50 MeV or less) has certainly not had the space it deserves; however, in this energy region intricate problems connected with diffraction and distortion are encountered which seem to be absent or at least unimportant above 150 MeV (100, 101). Nor have we surveyed the studies of quasi-free scattering effects on nucleon clusters such as high energy (p,pd), $(p,p\alpha)$, and $(\alpha,2\alpha)$ reactions which have been performed (30–40) and discussed (70, 117–123). For these reactions a correct treatment of the antisymmetrization requirement is important (119, 120) and the strong absorption of the composite outgoing particle necessitates a careful choice of the scattering geometry (121). Just as the $(p,2p)$ and (e,ep) reactions yield important information on the single-proton properties of the target nucleus, we expect to learn much about nucleon clustering and similar correlation effects from the (p,pd), $(p,p\alpha)$, and $(\alpha,2\alpha)$ reactions.

Summing up, we feel that the study of quasi-free scattering reactions of various kinds, performed with improved angular and energy resolution, will increase in importance as a source of nuclear information and will continue to stimulate the theoretical work on nuclear structure and on nuclear reaction mechanisms.

LITERATURE CITED

1. Chamberlain, O., and Segrè, E., *Phys. Rev.*, **87**, 81 (1952)
2. Cladis, J. B., Hess, W. N., and Moyer, B. J., *Phys. Rev.*, **87**, 425 (1952)
3. Wilcox, J. M., and Moyer, B. J., *Phys. Rev.*, **99**, 875 (1955)
4. Tyrén, H., Maris, Th. A. J., and Hillman, P., *Nuovo Cimento*, **6**, 1507 (1957)
5. Maris, Th. A. J., Hillman, P., and Tyrén, H., *Nucl. Phys.*, **7**, 1 (1958)
6. Tyrén, H., Hillman, P., Isacsson, P., and Maris, Th. A. J. (Reported by Jacob, G.), *Proc. Intern. Conf. Nucl. Struct., Kingston, July 1960*, 429
7. Tyrén, H., and Isacsson, P., *Proc. Natl. Conf. Nucl. Reactions Low Medium Energies, 2nd, Moscow, July 1960*, 274
8. Tyrén, H., Kullander, S., and Ramachandran, R., *Proc. Conf. Direct Interactions Nucl. Reaction Mech., Padua, Sept. 1962*, 1109
9. Tyrén, H., Kullander, S., Sundberg, O., Ramachandran, R., and Isacsson, P., *Proc. Paris Intern. Conf. Nucl. Struct., July 1964*, **II**, 334
10. Tyrén, H., Kullander, S., Sundberg, O., Ramachandran, R., Isacsson, P., and Berggren, T., *Nucl. Phys.*, **79**, 321 (1966)
11. Gottschalk, B., and Strauch, K., *Phys. Rev.*, **120**, 1005 (1960)
12. Gottschalk, B. (Ph.D. thesis, Harvard Univ., Cambridge, Mass., 1962) (Unpublished)
13. Gottschalk, B., Strauch, K., and Wang, K. H., *Proc. Paris Intern. Conf. Nucl. Struct., July 1964*, **II**, 324
14. Gooding, T. J., and Pugh, H. G., *Nucl. Phys.*, **18**, 46 (1960)
15. Pugh, H. G., and Riley, K. F., *Proc. Rutherford Jubilee Conf., Manchester, 1961*, 195
16. Garron, J. P., Jacmart, J. C., Riou, M., and Ruhla, Ch., *J. Phys. Radium*, **22**, 622 (1961)
17. Garron, J. P., Jacmart, J. C., Riou, M., Ruhla, Ch., Teillac, J., Caverzasio, C., and Strauch, K., *Phys. Rev. Letters*, **7**, 261 (1961)
18. Garron, J. P., Jacmart, J. C., Riou, M., Ruhla, Ch., Teillac, J., and Strauch, K., *Nucl. Phys.*, **37**, 126 (1962)
19. Garron, J. P., *Ann. Phys. (Paris)*, **7**, 301 (1962)
20. Ruhla, Ch., Riou, M., Ricci, R. A., Arditi, M., Doubre, H., Jacmart, J. C., Liu, M., and Valentin, L., *Phys. Letters*, **10**, 326 (1964)
21. Ruhla, Ch., Riou, M., Ricci, R. A., Arditi, M., Doubre, H., Jacmart, J. C., Liu, M., and Valentin, L., *Proc. Paris Intern. Conf. Nucl. Struct., July 1964*, **II**, 346
22. Roynette, J. C., Ruhla, Ch., Arditi, M., Jacmart, J. C., and Riou, M., *Phys. Letters*, **19**, 497 (1965)
23. Arditi, M., Roynette, J. C., Ruhla, Ch., Jacmart, J. C., Mazloum, F., and Riou, M. (Preprint, 1966)
24. Tyrén, H., Hillman, P., and Maris, Th. A. J., *Nucl. Phys.*, **7**, 10 (1958)
25. Hillman, P., Tyrén, H., and Maris, Th. A. J., *Phys. Rev. Letters*, **5**, 107 (1960)
26. Tibell, G., Sundberg, O., and Miklavžič, U., *Phys. Letters*, **1**, 172 (1962)
27. Tibell, G., Sundberg, O., and Miklavžič, U., *Phys. Letters*, **2**, 100 (1962)
28. Tibell, G., Sundberg, O., and Miklavžič, U., *Proc. Conf. Direct Interactions Nucl. Reaction Mech., Padua, Sept. 1962*, 1134
29. Tibell, G., Sundberg, O., and Renberg, P. U., *Arkiv Fysik*, **25**, 433 (1963)
30. Ruhla, Ch., Riou, M., Garron, J. P., Jacmart, J. C., and Massonet, L., *Phys. Letters*, **2**, 44 (1962)
31. Ruhla, Ch., Riou, M., Gusakov, M., Jacmart, J. C., Liu, M., and Valentin, L., *Phys. Letters*, **6**, 282 (1963)
32. Devins, D. W., Forster, H. H., Bunch, S. M., and Kim, C. C., *Phys. Letters*, **9**, 35 (1964)
33. Devins, D. W., Forster, H. H., and Scott, B. L., *Rev. Mod. Phys.*, **37**, 396 (1965)
34. Cuer, P., *Phys. Rev.*, **80**, 906 (1950)
35. Cuer, P., Combe, J., and Samman, A., *Compt. Rend.*, **240**, 25 (1955)
36. Samman, A., and Cuer, P., *J. Phys. Radium*, **19**, 13 (1958)
37. Gauvin, H., Chastel, R., and Vigneron, L., *Compt. Rend.*, **253**, 257 (1961)
38. James, A. N., and Pugh, H. G., *Nucl. Phys.*, **42**, 441 (1963)
39. Yuasa, T., and Hourani, E., *Rev. Mod. Phys.*, **37**, 399 (1965)
40. Igo, G., Hansen, L. F., and Gooding, T. J., *Phys. Rev.*, **131**, 337 (1963)

41. Chew, G. F., *Phys. Rev.*, **80**, 196 (1950)
42. Chew, G. F., and Goldberger, M. L., *Phys. Rev.*, **87**, 778 (1952)
43. Maris, Th. A. J., *Nucl. Phys.*, **9**, 577 (1958/59)
44. Berggren, T., Brown, G. E., and Jacob, G., *Phys. Letters*, **1**, 88 (1962)
45. Fernbach, S., Serber, R., and Taylor, T. B., *Phys. Rev.*, **75**, 1352 (1949)
46. Riou, M., *Rev. Mod. Phys.*, **37**, 375 (1965)
47. Jacob, G., and Maris, Th. A. J., *Rev. Mod. Phys.*, **38**, 121 (1966)
48. Clegg, A. B., *High Energy Nuclear Reactions*, 85 (Clarendon Press: Oxford Univ. Press, Oxford, 130 pp., 1965)
49. Bowden, A. R., Bowman, M. R., and Yuasa, T., *Proc. Paris Intern. Conf. Nucl. Struct., July 1964*, **II**, 331
50. Jacob, G., and Maris, Th. A. J., *Nucl. Phys.*, **31**, 139 and 152 (1962)
51. Johansson, A., *Phys. Rev.*, **136**, B1030 (1964)
52. Amaldi, U., Jr., Campos Venuti, G., Cortellessa, G., Fronterotta, C., Reale, A., Salvadori, P., and Hillman, P., *Proc. Paris Intern. Conf. Nucl. Struct., July 1964*, 341
53. Amaldi, U., Jr., Campos Venuti, G., Cortellessa, G., Fronterotta, C., Reale, A., Salvadori, P., and Hillman, P., *Phys. Rev. Letters*, **13**, 341 (1964)
54. Campos Venuti, G., and Salvadori, P. (Preprint 1965)
55. Amaldi, U., Jr., Campos Venuti, G., Cortellessa, G., Fronterotta, C., Reale, A., and Salvadore, P., *Atti Accad. Nazl. Lincei, Rend., Classe Sci. Fis. Mat. Nat.*, **38**, 499 (1965)
56. Mayer, M. G., and Jensen, J. H. P., *Elementary Theory of Nuclear Shell Structure* (Wiley, New York, 1955)
57. Goldhammer, P., *Rev. Mod. Phys.*, **35**, 40 (1963)
58. Glendenning, N. K., *Ann. Rev. Nucl. Sci.*, **13**, 191 (1963)
59. Racah, G., *Phys. Rev.*, **63**, 367 (1943)
60. Jahn, H. A., and van Wieringen, H., *Proc. Roy. Soc. (London)*, **A209**, 502 (1951)
61. Edmonds, A. R., and Flowers, B. H., *Proc. Roy. Soc. (London)*, **A214**, 515 (1952)
62. Flowers, B. H., *Proc. Roy. Soc. (London)*, **A215**, 398 (1952)
63. Elliot, J. P., Hope, J., and Jahn, H. A., *Phil. Trans.*, **A246**, 241 (1953)
64. Jahn, H. A., *Phys. Rev.*, 96, 989 (1954)
65. Balashov, V. V., *J. Exptl. Theoret. Phys. (USSR)*, **36**, 1387 (1959); Transl. *Soviet Phys. JETP*, **9**, 988 (1959)
66. Glaudemans, P. W. M., Wiechers, G., and Brussaard, J. P., *Nucl. Phys.*, **56**, 529 (1964)
67. Dietrich, K., *Phys. Letters*, **2**, 139 (1962)
68. Benioff, P. A., *Nucl. Phys.*, **26**, 68 (1961)
69. Balashov, V. V., and Boyarkina, A. N., *Nucl. Phys.*, **38**, 629 (1962)
70. Balashov, V. V., Boyarkina, A. N., and Rotter, I., *Nucl. Phys.*, **59**, 417 (1964)
71. Rosenblum, W. M. (Master's thesis, Florida State Univ., Tallahassee, Fla., 1960) (Unpublished)
72. Riley, K. F., *Nucl. Phys.*, **13**, 3 (1959)
73. Riley, K. F., Pugh, H. G., and Gooding, T. J., *Nucl. Phys.*, **18**, 65 (1960)
74. Sakamoto, Y., *Phys. Letters*, **1**, 256 (1962)
75. Berggren, T., and Jacob, G., *Phys. Letters*, **1**, 258 (1962)
76. Berggren, T., and Jacob, G., *Proc. Intern. Conf. Direct Interactions Nucl. Reaction Mech., Padua, Sept. 1962*, 38
77. Sakamoto, Y., *Nuovo Cimento*, **26**, 461 (1962)
78. Sakamoto, Y., *Progr. Theoret. Phys., (Kyoto)*, **28**, 803 (1962)
79. Johansson, A., and Sakamoto, Y., *Nucl. Phys.*, **42**, 625 (1963)
80. Lim, K. L., and McCarthy, I. E., *Phys. Rev. Letters*, **10**, 529 (1963)
81. Berggren, T., and Jacob, G., *Nucl. Phys.*, **47**, 481 (1963)
82. Lim, K. L., and McCarthy, I. E., *Phys. Rev.*, **133**, B1006 (1964)
83. Lipkin, H. J., *Phys. Rev.*, **110**, 1395 (1958)
84. Berggren, T., *Nucl. Phys.*, **72**, 337 (1965)
85. Pinkston, W. T., and Satchler, G. R., *Nucl. Phys.*, **72**, 641 (1965)
86. Bolsterli, M., *Phys. Rev.*, 129, 2830 (1963)
87. Austern, N., *Phys. Rev.*, **136**, B1743 (1964)
88. Tang, Y. C., Wildermuth, K., and Pearlstein, L. D., *Phys. Rev.*, **123**, 548 (1961)
89. Tang, Y. C., Wildermuth, K., and Pearlstein, L. D., *Nucl. Phys.*, **32**, 504 (1962)
90. Maris, Th. A. J., *Proc. Intern. Conf. Direct Interactions Nucl. Reaction Mech., Padua, Sept. 1962*, 31

91. Humblet, J., and Rosenfeld, L., *Nucl. Phys.*, **26,** 529 (1961)
92. Brink, D. M., and Sherman, N., *Phys. Rev. Letters*, **14,** 393 (1965)
93. Lippmann, B., and Schwinger, J., *Phys. Rev.*, **79,** 469 (1950)
94. Gell-Mann, M., and Goldberger, M. L., *Phys. Rev.*, **91,** 398 (1953)
95. Kerman, A. K., McManus, H., and Thaler, R. M., *Ann. Phys. (N.Y.)*, **8,** 551 (1959)
96. Greider, K. R., *Phys. Rev.*, **114,** 786 (1959)
97. Jackson, D. F., and Berggren, T., *Nucl. Phys.*, **62,** 353 (1965)
98. Jackson, D. F., *Nucl. Phys.* (To be published)
99. Maris, Th. A. J. (Private communication)
100. Lim, K. L., and McCarthy, I. E., *Phys. Rev. Letters*, **13,** 446 (1964)
101. Lim, K. L., and McCarthy, I. E. (Preprint)
102. McCarthy, I. E., *Rev. Mod. Phys.*, **37,** 388 (1965)
103. Watson, K. M., *Phys. Rev.*, **89,** 575 (1953)
104. McCauley, G. P., and Brown, G. E., *Proc. Phys. Soc. (London)*, **71,** 893 (1958)
105. McCarthy, I. E., Jezak, E. V., and Krominga, A. J., *Nucl. Phys.*, **12,** 274 (1959)
106. McCarthy, I. E., and Krominga, A. J., *Phys. Rev. Letters*, **4,** 288 (1960)
107. Jacob, G., and Maris, Th. A. J., *Phys. Rev. Letters*, **5,** 210 (1960)
108. Jacob, G., and Maris, Th. A. J., *Nucl. Phys.*, **20,** 440 (1960)
109. McCarthy, I. E., *Proc. Intern. Conf. Direct Interactions Nucl. Reaction Mech., Padua, Sept. 1962*, 94
110. Benioff, P. A., *Phys. Rev.*, **119,** 324 (1960)
111. Benioff, P. A., *Phys. Rev.*, **129,** 1355 (1963)
112. Sakamoto, Y., *Nucl. Phys.*, **46,** 293 (1963)
113. Cohen, B. L., *Phys. Rev.*, **108,** 768 (1957)
114. Griffiths, R. J., and Eisberg, R. M., *Nucl. Phys.*, **12,** 225 (1959)
115. Pugh, H. G., Hendrie, D. L., Chabre, M., and Boschitz, E., *Phys. Rev. Letters*, **14,** 434 (1965)
116. Gibson, W. R., Johnston, A. R., and Griffiths, R. J., *Nucl. Phys.*, **70,** 114 (1965)
117. Sakamoto, Y., *Nuovo Cimento*, **28,** 206 (1963)
118. Sakamoto, Y., *Phys. Rev.*, **134,** B1211 (1964)
119. Jackson, D. F., and Elton, L. R. B., *Proc. Phys. Soc. (London)*, **85,** 659 (1965)
120. Jackson, D. F., *Rev. Mod. Phys.*, **37,** 393 (1965)
121. Jackson, D. F., *Nuovo Cimento*, **40B,** 109 (1965)
122. Jackson, D. F., *Proc. Phys. Soc. (London)* (To be published)
123. Beregei, P., Selenškaja, N. S., Neudatchin, V. G., and Smirnov, Yu. F. *Proc. Paris Intern. Conf. Nucl. Struct., July 1964*, **II,** 319